Similarity of Fluorescence Lifetime Distributions for Single Tryptophan Proteins in the Random Coil State

R. Swaminathan, G. Krishnamoorthy, and N. Periasamy

Chemical Physics Group, Tata Institute of Fundamental Research, Homi Bhabha Road, Colaba, Bombay 400 005, India

ABSTRACT   The picosecond time-resolved fluorescence decay data of nine single-tryptophan (trp) proteins and two multi-trp proteins in their native and denatured states were analyzed by the maximum entropy method (MEM). In the denatured state (6 M guanidine hydrochloride) a majority of the single-trp proteins show bimodal (at 25°C) and trimodal (at 85°C) distributions with similar patterns and similar values for average lifetimes. In the native state of the proteins the lifetime distributions were bimodal or trimodal. These results (multimodal distributions) are contradictory to the unimodal Lorentzian distribution of lifetimes reported for some proteins in the native and denatured states. MEM analysis gives a unimodal distribution of lifetimes only when the signal-to-noise ratio is poor in the time-resolved fluorescence decay data. The unimodal distribution model is therefore not realistic for proteins in the native and denatured states. The fluorescence decay components of the bi- or trimodal distribution are associated with the rotamer structures of the indole moiety when the protein is in the random coil state.

INTRODUCTION

The intrinsic fluorescence of proteins due to tryptophan (trp) residues is a valuable spectroscopic property for probing the structure and dynamics of the protein. The fluorescence parameters (quantum yield, absorption and emission spectra, fluorescence, and anisotropy decay parameters) of the indole chromophore in trp are highly sensitive toward the local environment and hence its usefulness as a probe of local structure and dynamics (Weber, 1953; Lumry and Hershberger, 1978; Creed, 1984; Lakowicz, 1983; Eftink, 1991). However, the very same sensitivity makes it difficult to interpret the fluorescence data of proteins if various possibilities for the local structure of indole exist. There exists a broad consensus for associating the absorption and emission spectral peak positions and peak shifts of the trp residue to the properties of the local environment in terms of polarity, hydrophobicity, or hydrophilicity (Lakowicz, 1983; Demchenko, 1992). Such a consensus does not exist for the association of other fluorescence parameters, especially those related to the decays of fluorescence and anisotropy with the structure and dynamics. This leads to a situation where identical or similar experimental results are interpreted differently.

A problem that has been discussed extensively concerns the origin of the two fluorescence lifetimes (~0.5 and ~3.1 ns) for trp in water at pH 7, whereas the fluorescence decay of indole or N-acetyl tryptophanamide (NATA) is a single exponential (Beechem and Brand, 1985). One interpretation is based on the structural heterogeneity in the ground state of trp where the local environment (and hence the fluorescence property) of the indole chromophore differs substantially (Szabo and Rayner, 1980; Chang et al., 1983; Petrich et al., 1983). The principal structural heterogeneity in trp is

associated with the three rotamer structures about the C_α—C_β bond, which are long-lived (ms timescale (Ross et al., 1992)) compared with the ns timescale of the excited state of indole. The short lifetime component is associated with the two rotamers in which indole is closer to the carboxyl group. An alternative model associates the short lifetime component with the unrelaxed excited state of indole and the long component with the relaxed exciplex state. This model requires that the preexponential for the short lifetime component to be negative, which has been experimentally observed (Vekshin et al., 1992).

The intrinsic fluorescence decay due to trp in several proteins is known to be multiexponential. The fluorescence decay characteristics at room temperature vary widely even for proteins containing only one trp. The experimentally measured lifetimes vary from 0.014 to 9.8 ns (Beechem and Brand, 1985; Tanaka and Mataga, 1992). Neither the rotamer model nor the exciplex model can explain satisfactorily the widely varying lifetimes for the indole chromophore in the proteins in the native state. In the case of proteins it is necessary to assess the importance of the multiple conformations (microstates) of the protein, which is an additional source of heterogeneity and multiple lifetimes. It will be desirable to establish some experimental conditions where the fluorescence properties of trps in all proteins behave similarly.

Intuitively, one would expect that the fluorescence characteristics of trp to be similar in the random coil state of the protein. Grinvald and Steinberg (1976) found the fluorescence decay of the trp residue is a two exponential in the random coil state, and the lifetimes and amplitudes were nearly the same for several proteins. In recent times it has been believed that the lifetimes are likely to be distributed continuously in proteins and polypeptides (Alcala et al., 1987a,b; Rosato et al., 1990). Analysis of fluorescence decay data has shown that the distribution is unimodal in the random coil state of the protein (Bismuto et al., 1988; Fernando and Royer, 1992), and the width of the distribution increases with the chain length (Bismuto et al., 1991).

In this paper we report the experimental results of the analysis of fluorescence decays of several proteins containing one or more trps in the random coil states and in their native states. The application of maximum entropy method (MEM) to the analysis of the fluorescence decays showed that the distribution is multimodal for the protein in the native and denatured state. The fluorescence lifetime distributions of most proteins are similar in the random coil state. The results support the rotamer model in the random coil state.

MATERIALS AND METHODS

Superoxide dismutase (SOD, human erythrocytes), human albumin, ribonuclease T1 (RNase T1, *Aspergillus oryzae*), glucagon (mixture of bovine and porcine pancreas), melittin (bee venom), protease subtilisin Carlsberg (bacterial), monellin (*Dioscoreophyllum cumminsii*), myelin basic protein (bovine brain), and lysozyme (chicken egg white) of the highest available purity were purchased from Sigma Chemical Co. (St. Louis, MO) and used without further treatment. The emission spectra of all proteins excited at 295 nm are attributable to trp only. The fluorescence lifetimes obtained in our experiments by the discrete analysis (see Table 1, first row) were compared with values reported in literature under similar conditions (25°C and pH 7) for the same proteins (obtained, however, from a different source). The mean lifetimes calculated (according to the equation $\tau_m = \sum_i \alpha_i \tau_i / \sum_i \alpha_i$) from the reported values for human albumin (3.57 ns), RNase T1 (2.83 ns), glucagon (2.22 ns) and lysozyme (1.48 ns) (Grinvald and Steinberg, 1976) are in good agreement with our values. However, the mean lifetime calculated for subtilisin Carlsberg (2.82 ns) is significantly different from our value (2.10 ns). The cyclic hexapeptide, -His-Gly-Gly-Trp-Arg-Phe- (HPLC purified), was kindly donated by Prof. Anil Saran, Tata Institute of Fundamental Research, Bombay. Barstar was obtained from a bacterial overexpression system described elsewhere (Swaminathan et al., 1994). Guanidine hydrochloride (GdnHCl) (molecular biology reagent grade) was obtained from Sigma Chemical Co. Samples were made in deionized water. All other chemicals used were of Analar grade.

Experiments in the presence of denaturant were carried out at least 12 h after the addition of the denaturant to allow for complete unfolding of the protein. Other details regarding experimental conditions are given in the figure legends.

Time-resolved fluorescence decays of the samples were measured using a time-correlated single photon-counting experimental setup described previously (Periasamy et al., 1988; Banker et al., 1989). The setup uses a continuous wave mode-locked, frequency-doubled Nd-YAG laser-driven, cavity-dumped Rhodamine 6G dye laser operating at a repetition rate of 800 kHz. All samples were excited by 295-nm pulse obtained by frequency doubling the 10 ps-wide dye laser pulse at 590 nm. The full width of the instrument response function is 80–100 ps using microchannel plate photomultiplier (R2809, Hamamatsu Corp., Toyooka, Japan). Fluorescence emission was collected through a 320-nm cut-off filter to exclude scattered photons completely when the monochromator was set at 340 or 360 nm. Use of a polarizer oriented at the magic angle (54.7°) eliminates anisotropy decay artifact in the fluorescence decay data. The fluorescence decays were collected at a time resolution of 37.8 ps/channel. The peak count in the fluorescence decay is between 15 and 20 × 10³ counts, unless stated otherwise. The emission wavelength was kept between 340 and 360 nm for observation of proteins in the native state. For denatured proteins the emission was observed at 360 nm. Protein concentrations were typically 250 μM for single-trp proteins and 100 μM for multi-trp proteins. The control samples, without the proteins, were fluorescence free.

Steady-state fluorescence spectra of all the samples were recorded using a spectrofluorimeter (model RF-540, Shimadzu Scientific Instruments, Kyoto, Japan).

Fluorescence decay analysis

Experimentally measured time-resolved fluorescence decay data, $F(t)$, is a convolution of the instrument response function, $R(t)$, and the intensity decay function of the sample, $I(t)$:

$$F(t) = \int_0^t R(s + \delta)I(t - s)\,ds \tag{1}$$

where δ is the shift parameter, which is a fraction of the time per channel. $R(t)$ is experimentally determined. $I(t)$ is a function assumed to describe the fluorescence dynamics of the sample. Decay data analysis involves the determination of the best values for the unknown parameters in $I(t)$.

Time-resolved fluorescence decay data were fitted to a function that is a sum of discrete exponentials,

$$I(t) = \sum_i \alpha_i \exp\left(-\frac{t}{\tau_i}\right), \tag{2}$$

where $\sum_i \alpha_i = 1.0$, by the iterative reconvolution method (Grinvald and Steinberg, 1974). Correction factors for the parameters (α_i and τ_i) in successive iterations were determined by the application of Marquardt's method in nonlinear least-squares analysis (Bevington, 1969). Numerical calculation of the convolution integrals for intensity and partial derivatives were done using the Grinvald-Steinberg recursion equations (Grinvald and Steinberg, 1974). The mean lifetime $\tau_m = \sum_i \alpha_i \tau_i$.

Unimodal Lorentzian distribution of lifetimes is described by the following function for the intensity decay:

$$I(t) = \int_0^\infty \alpha(\tau)\exp\left(-\frac{t}{\tau}\right)d\tau \tag{3}$$

where

$$\alpha(\tau) = \left(\frac{2}{\Gamma}\right)\left[\frac{\pi}{2} + \tan^{-1}\left(\frac{2\tau_m}{\Gamma}\right)\right]^{-1} \times \left[1 + \frac{4(\tau - \tau_m)^2}{\Gamma^2}\right]^{-1} \tag{4}$$

where τ_m is the mean lifetime and Γ is the full width at half maximum. $\alpha(\tau)$ satisfies the property that $\int_0^\infty \alpha(\tau)\,d\tau = 1.0$ and $\int_0^\infty \alpha(\tau)\,\tau\,d\tau = \tau_m$. Fitting of fluorescence decay data to Eq. 3 involves optimization of the values of τ_m and Γ. For the purpose of numerical calculations the integral in Eq. 3 is replaced by a sum,

$$I(t) = \sum_{i=1}^N \alpha_i \exp\left(-\frac{t}{i\Delta\tau}\right) \tag{5}$$

where $\Delta\tau$ is the interval in τ space. $\Delta\tau = 0.1$ ns for $N = 100$ for the range of τ from 0 to 10 ns. Optimization of the parameters follows the procedure identical to that adopted for the fit of multiexponential function.

MEM assumes that the lifetimes are distributed (Eq. 3) in a range of 10 ps–10 ns. The lower limit is a constraint imposed by the experimental technique used in this study, and the upper limit is the maximum lifetime for the chromophore indole experimentally observed (Beechem and Brand, 1985). The function $\alpha(\tau)$ describing the distribution is unknown, and a numerical representation for $\alpha(\tau)$ is obtained as the end result of MEM analysis. Following the procedural recommendations for MEM analysis (Livesey and Brochon, 1987), $I(t)$ is represented by N exponentials ($N = 150$) with lifetimes that are equally spaced in log τ space. The initial distribution of $\alpha(\tau)$ is chosen to be an unbiased one, namely a constant value of $(1/N)$ for all lifetimes. This distribution is the appropriate one for the decay data consisting of noise only. For this flat distribution the entropy, defined by Eq. 6, is maximum, and χ^2, defined by Eq. 7, is very high for fluorescence decay data.

$$S = -\sum_i \alpha_i \log \alpha_i \tag{6}$$

$$\chi^2 = \frac{(1/m)\sum_{i=1}^m [F_c(t_i) - F_e(t_i)]^2}{F_e(t_i)}. \tag{7}$$

In Eq. 6 α_i is normalized such that $\sum_i \alpha_i = 1.0$. $F_c(t_i)$ and $F_e(t_i)$ are the calculated and experimental fluorescence intensity at time t_i, and m is the number of data points. Data analysis consists of determining a correction vector for α_i in the N-dimensional space such that the new set of values of

α_i minimizes χ^2 and maximizes the entropy for that value of χ^2. The analysis continues in successive iterations until χ^2 is minimized to an acceptable value, usually 1.0, if there is no systematic noise in the fluorescence decay data. The correction vector for successive iterations is determined according to the general algorithm described by Skilling and Bryan (1984) for maximum entropy analysis. α_i values are constrained to be positive in the analysis. Positivity of α_i is enforced either by dividing the negative values by a constant so that negative values for α_i gradually disappear or by equating them to 0. The former procedure ensures that the final distribution is smooth.

The MEM method has been tested with several data sets for standard samples (NATA, trp, and fluorescent dyes) for which the fluorescence decay is either a single exponential or two exponentials. The MEM method was also tested using synthetic data sets for single- and double-exponential decay kinetics. It was found that the distribution in log τ space consists of a single peak (termed as unimodal distribution), and the shape is approximately gaussian if the data set belongs to a case of single exponential decay function. Interestingly, but not surprisingly, the full width at half maximum depends upon the signal-to-noise ratio (or peak count) in the data set (Swaminathan and Periasamy, unpublished). Similarly, for double exponential decay kinetics, MEM analysis generated a bimodal distribution with two peaks, each of which is again approximately gaussian (Swaminathan and Periasamy, unpublished). The resolvability of the peaks depended upon the signal-to-noise ratio. Distributions with multiple peaks were therefore resolved into a minimum number of gaussians by a nonlinear least-squares fitting program. For each resolved peak, mean lifetime, $\langle \tau_j \rangle$, and mean amplitude, $\langle \alpha_j \rangle$, were calculated as follows:

$$\langle \alpha_j \rangle = \sum_i \alpha_i \tag{8}$$

$$\langle \tau_j \rangle = \sum_i \alpha_i \tau_i \Big/ \sum_i \alpha_i \tag{9}$$

where α_i and τ_i refer to the points in the jth resolved peak. The global average lifetime (mean lifetime), τ_m is calculated using Eq. 10:

$$\tau_m = \sum_{i=1}^N \alpha_i \tau_i \Big/ \sum_{i=1}^N \alpha_i \tag{10}$$

The value of τ_m obtained by MEM and discrete exponential analysis are comparable.

RESULTS

The fluorescence decays of nine single-trp proteins (including cyclic hexapeptide) were obtained for three experimental conditions: native state at 25°C, denatured state (in the presence of 6 M GdnHCl) at 25 and 85°C. The decay data were analyzed by MEM to fit to a distribution of lifetimes and by Marquardt's method to fit to a sum of exponentials.

Fig. 1, A and B, shows the raw fluorescence decay data of melittin (3 kDa) and human albumin (64 kDa) for the three experimental conditions: native state at 25°C (N), denatured state at 25°C (D), and heat denatured at 85°C (HD). While the fluorescence decay of the relatively small-sized melittin is only moderately affected by the denaturant at 25°C, the change in the decay profile is very substantial in the case of human albumin. The fluorescence decays of melittin and human albumin are similar in the presence of denaturant. The decay profiles become virtually identical at 85°C in the presence of the denaturant. The substantial quenching of fluorescence at 85°C in both the cases is largely a temperature effect. The shapes of the fluorescence decays of other proteins are also similar at 25°C and nearly identical at 85°C to those of melittin and human albumin in the presence of the
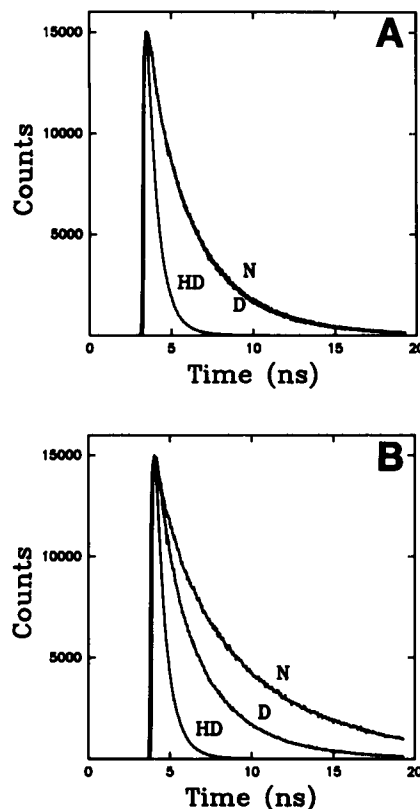

FIGURE 1   (A) Fluorescence intensity decay of melittin. Native (N) in 10 mM Tris, 1 mM EDTA, pH 7.0 at 25°C; denatured (D) in 10 mM NaH$_2$PO$_4$, 1 mM EDTA, 6 M GdnHCl, pH 7.0 at 25°C; heat denatured (HD) in 10 mM NaH$_2$PO$_4$, 1 mM EDTA, 6 M GdnHCl at 85°C. Tris buffer was used in the native condition (N) to prevent the formation of melittin tetramer. Excitation was at 295 nm, and emission was observed at 360 nm for all conditions. The decay parameters for N, D, and HD are given in Tables 1, 2, and 3, respectively. See Materials and Methods for other details. (B) Fluorescence intensity decay of human albumin. Native (N) in 10 mM NaH$_2$PO$_4$, 1 mM EDTA, pH 7.0 at 25°C; decays (D) and (HD) stand for the same conditions as mentioned in (A). Excitation was at 295 nm, and emission was observed at 340 nm for N and at 360 nm for D and HD. The decay parameters for N, D and HD are given in Tables 1, 2, and 3, respectively. See Materials and Methods for other details.

denaturant. The differences in the fluorescence decay profiles in the native state and the similarity of the profiles in the denatured state are revealed in the quantitative analysis of the data by MEM. Fig. 2, $A–C$, show the distributions of lifetimes obtained for the best MEM fit of the fluorescence decays of nine single-trp proteins in the native (25°C, pH 7), denatured (25°C, pH 7, 6 M GdnHCl), and heat-denatured (85°C, 6 M GdnHCl) conditions, respectively. The distribution is either bimodal or trimodal in the native state. In the presence of denaturant the distribution is bimodal at 25°C (except monellin) and trimodal at 85°C (except SOD). Inspection of Fig. 2, $A–C$ shows that the distribution profiles that vary widely for the nine proteins in their native states become similar in the presence of 6 M GdnHCl at 25 and 85°C.

The numerical results of the distributions for all proteins for the three conditions are collected together in Tables 1–3.
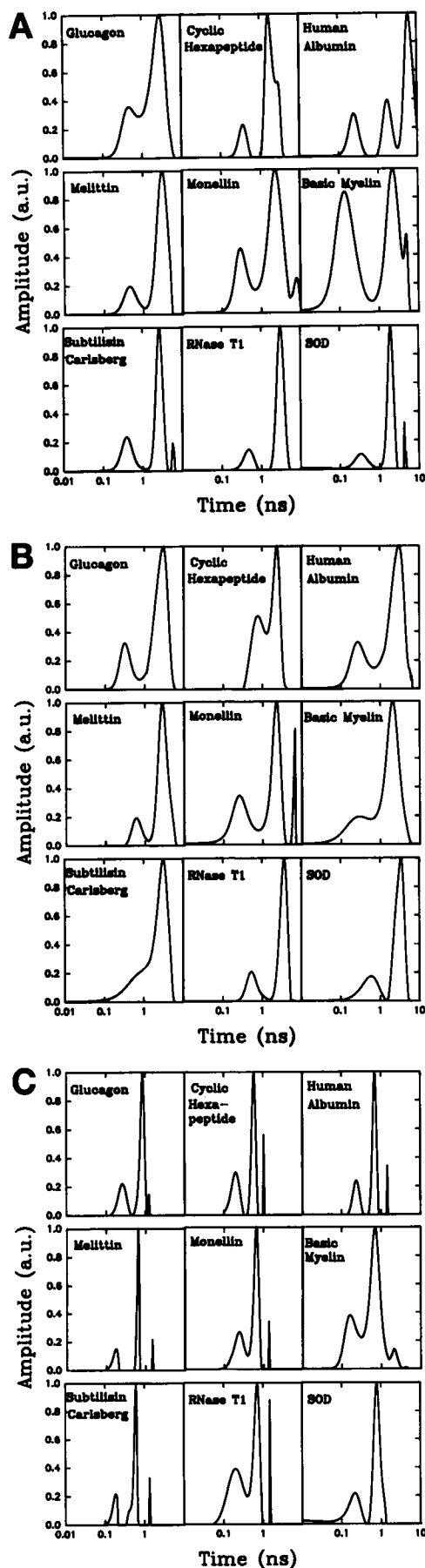
The average lifetimes and amplitudes of the individual peaks of the bi- or trimodal distributions and the global average lifetime, τ_m, were calculated as outlined in Materials and Methods. All fluorescence decays were also fitted to a sum of two or three exponentials. The fact that the fluorescence decay data is adequately fitted in MEM and discrete exponential analysis is revealed in the low χ^2 values and non-random distribution of weighted residuals and autocorrelation function values in each case. Fig. 3 shows the distributions of weighted residuals and autocorrelation function values obtained in fitting the raw decay data of melittin. Fig. 3 also shows the distributions of weighted residuals and autocorrelation function values obtained in fitting the raw data to a sum of three exponentials. The randomness of the distributions of residuals and autocorrelation function values indicates that the decay functions are adequate to fit the experimental fluorescence decay data. It is to be noted that the distribution of lifetimes at 25°C is bimodal, whereas in discrete exponential analysis a three-exponential function was giving better fits. The results of the discrete exponential analysis are also given in Tables 1–3. In those cases where a two-exponential function was adequate, only two values for lifetimes and amplitudes are given. The values for the decay parameters given in Tables 1–3 for the same protein are averages of two measurements. The shapes of the distributions shown in Fig. 2, *A–C*, and the numerical results are reproducible in repeat experiments within 10% error in the average lifetimes and amplitudes.

The fluorescence decays of two multi-trp proteins, lysozyme and barstar, were also obtained for the three experimental conditions for comparison with the results of single-trp proteins. These show bimodal (barstar) or trimodal (lysozyme) distributions in their native state and bimodal distributions in the denatured state at 25°C and trimodal distribution at 85°C (profiles not shown). The results for these proteins are also included in Tables 1–3. The distribution profiles at 25 and 85°C are approximately similar to those in Fig. 2, *B* and *C*.

DISCUSSION

The analysis of fluorescence decays was carried out by two methods. The conventional method of fitting the fluores-

FIGURE 2   (*A*) Fluorescence lifetime distributions of native proteins containing a single trp. All observations were made at 25°C, in 10 mM NaH_2PO_4, 1 mM EDTA, pH 7.0 except in the case of melittin where the sample contained 10 mM Tris, 1 mM EDTA, pH 7.0 to prevent the formation of melittin tetramer. Excitation was at 295 nm and emission was observed between 340 and 360 nm for all proteins. See Materials and Methods for other experimental details. (*B*) Fluorescence lifetime distributions of denatured proteins containing a single trp at 25°C in 10 mM NaH_2PO_4, 1 mM EDTA, 6 M GdnHCl, pH 7.0. Excitation was at 295 nm and emission was observed at 360 nm in all cases. See Materials and Methods for other experimental details. (*C*) Fluorescence lifetime distributions of heat-denatured proteins containing a single trp at 85°C in 10 mM NaH_2PO_4, 1 mM EDTA, and 6 M GdnHCl. Excitation was at 295 nm and emission was observed at 360 nm in all cases. See Materials and Methods for other experimental details.

TABLE 1   Parameters obtained at 25°C from the analysis of fluorescence intensity decays of single- and multi-trp proteins

Protein*	Lifetimes (ns)			Amplitudes			$\tau_m^{\ddagger}$ (ns)	χ^2_{red}
	τ_1	τ_2	τ_3	α_1	α_2	α_3		
Glucagon	3.64	1.56	0.30	0.32	0.39	0.28	1.88	0.97
	3.19	1.99	0.53	0.37	0.35	0.28	2.03	1.06
Cyclic hexapeptide	2.85	1.62	0.36	0.28	0.56	0.16	1.76	1.12
	2.85	1.73	0.37	0.23	0.61	0.16	1.78	1.12
Human albumin	6.55	1.95	0.17	0.46	0.23	0.31	3.48	1.09
	6.23	1.78	0.25	0.57	0.23	0.20	4.02	1.14
Melittin	4.32	2.29	0.34	0.29	0.48	0.22	2.45	1.00
	3.16		0.51	0.80		0.20	2.63	1.00
Monellin	5.35	1.94	0.34	0.18	0.52	0.30	2.08	1.17
	7.77	2.49	0.35	0.05	0.66	0.29	2.11	1.16
Basic myelin	3.93	1.71	0.20	0.20	0.34	0.46	1.46	1.16
	4.91	2.42	0.16	0.04	0.43	0.53	1.31	1.21
Subtilisin Carlsberg	4.64	2.42	0.35	0.13	0.58	0.29	2.10	1.06
	5.85	2.71	0.42	0.04	0.68	0.28	2.21	1.09
Ribonuclease T$_1$	3.32	1.18		0.77	0.23		2.82	1.36
	3.11	0.49		0.84	0.16		2.68	1.07
Superoxide dismutase	3.60	1.78	0.31	0.10	0.71	0.19	1.68	1.12
	4.19	1.91	0.36	0.04	0.78	0.18	1.71	1.11
Lysozyme	3.65	1.67	0.37	0.12	0.59	0.29	1.53	1.09
	4.25	1.88	0.44	0.06	0.61	0.33	1.54	1.09
Barstar	4.12	1.42		0.47	0.53		2.69	1.23
	3.73	1.38		0.55	0.45		2.68	1.12

The decays were fitted to a sum of exponentials and to a distribution of lifetimes using the MEM. The parameters obtained from the discrete exponential fit and the distribution fit are given in the first and second row, respectively. See the legend to Fig. 2 A for experimental details and Materials and Methods for the technique.

* With the exception of lysozyme and barstar, the rest of the proteins possess only one trp residue.

$\ddagger$ Mean lifetime $= \sum_{i=1}^{N} \alpha_i \tau_i / \sum_{i=1}^{N} \alpha_i$, where N is 2 or 3 for discrete exponential fit and $N = 150$ for distribution fit.

TABLE 2   Parameters obtained at 25°C (in 6 M GdnHCl) from the analysis of fluorescence intensity decays of single- and multi-trp proteins

Protein*	Lifetimes (ns)			Amplitudes			$\tau_m^{\ddagger}$ (ns)	χ^2_{red}
	τ_1	τ_2	τ_3	α_1	α_2	α_3		
Glucagon	3.50	1.66	0.26	0.40	0.36	0.24	2.06	1.21
	2.88		0.35	0.76		0.24	2.28	1.22
Cyclic hexapeptide	2.58	1.26	0.42	0.34	0.42	0.24	1.51	0.92
	2.34		0.93	0.46		0.54	1.58	1.02
Human albumin	3.70	1.61	0.24	0.35	0.37	0.28	1.96	1.06
	2.92		0.41	0.66		0.34	2.08	1.18
Melittin	4.07	2.27	0.39	0.30	0.50	0.20	2.43	1.05
	2.95		0.64		0.83	0.17	2.56	1.13
Monellin	5.22	1.87	0.29	0.15	0.51	0.34	1.85	1.12
	6.36	2.23	0.33	0.08	0.53	0.39	1.83	1.10
Basic myelin	3.50	1.72	0.45	0.20	0.58	0.23	1.78	0.95
		2.18	0.64		0.63	0.37	1.60	1.05
Subtilisin Carlsberg	3.92	2.07	0.58	0.35	0.44	0.22	2.40	0.96
	3.22	1.49		0.56	0.44		2.47	1.00
Ribonuclease T$_1$	3.88	2.12	0.40	0.53	0.24	0.23	2.66	1.19
	3.56		0.57	0.77		0.23	2.86	1.23
Superoxide dismutase	3.93	2.50	0.49	0.30	0.50	0.20	2.52	1.10
	3.17		0.60	0.75		0.25	2.53	1.01
Lysozyme	3.34	1.49	0.28	0.31	0.37	0.32	1.66	1.27
	2.88	1.17		0.40	0.60		1.86	1.30
Barstar	3.54	1.26		0.55	0.45		2.51	1.20
	3.36	1.62		0.49	0.51		2.48	1.04

The decays were fitted to a sum of exponentials and to a distribution of lifetimes using the MEM. The parameters obtained from the discrete exponential fit and the distribution fit are given in the first and second row, respectively. See the legend to Fig. 2 B for experimental details and Materials and Methods for the technique.

* With the exception of lysozyme and barstar, the rest of the proteins possess only one trp residue.

$\ddagger$ Mean lifetime $= \sum_{i=1}^{N} \alpha_i \tau_i / \sum_{i=1}^{N} \alpha_i$, where N is 2 or 3 for discrete exponential fit and $N = 150$ for distribution fit.

cence decay data to a sum of discrete exponentials assumes that the fluorophore is heterogeneously distributed in two or more spectroscopically distinct environments/structures and the interconversion among them is far slower than the fluorescence decay rate. It is usually believed that this method cannot detect four or more decay components especially if

TABLE 3   Parameters obtained at 85°C (in 6 M GdnHCl) from the analysis of fluorescence intensity decays of single- and multi-trp proteins

Protein*	Lifetimes (ns)			Amplitudes			$\tau_m{}^{\ddagger}$ (ns)	χ^2_{red}
	τ_1	τ_2	τ_3	α_1	α_2	α_3		
Glucagon	1.10	0.77	0.22	0.13	0.57	0.30	0.65	1.23
	1.24	0.85	0.26	0.02	0.69	0.29	0.68	1.29
Cyclic hexapeptide	1.05	0.58	0.19	0.05	0.56	0.39	0.45	1.07
	1.03	0.58	0.20	0.05	0.59	0.36	0.47	1.09
Human albumin	1.59	0.68	0.22	0.03	0.66	0.31	0.56	1.24
	1.43	0.69	0.24	0.04	0.69	0.27	0.59	1.33
Melittin	1.66	0.65	0.15	0.03	0.64	0.33	0.52	0.96
	1.50	0.64	0.17	0.05	0.71	0.25	0.57	1.01
Monellin	1.29	0.63	0.23	0.04	0.62	0.34	0.52	1.07
	1.36	0.65	0.26	0.03	0.59	0.38	0.52	1.00
Basic myelin	2.06	0.71	0.20	0.07	0.57	0.36	0.62	1.20
	2.10	0.71	0.20	0.05	0.61	0.34	0.61	1.42
Subtilisin Carlsberg	1.49	0.60	0.18	0.03	0.64	0.32	0.49	1.13
	1.36	0.60	0.18	0.05	0.70	0.25	0.54	1.21
Ribonuclease T_1	1.30	0.62	0.19	0.09	0.50	0.42	0.50	1.06
	1.50	0.70	0.26	0.04	0.43	0.53	0.51	1.09
Superoxide dismutase	1.14	0.76	0.24	0.10	0.63	0.27	0.66	1.18
	1.12	0.77	0.21	0.04	0.69	0.27	0.63	1.17
Lysozyme	0.86	0.47	0.12	0.18	0.43	0.39	0.41	0.92
	0.70	0.38	0.06	0.25	0.35	0.40	0.33	1.10
Barstar	1.31	0.66	0.29	0.06	0.60	0.34	0.57	0.99
	1.51	0.75	0.38	0.02	0.40	0.49	0.58	1.08

The decays were fitted to a sum of exponentials and to a distribution of lifetimes using the MEM. The parameters obtained from the discrete exponential fit and the distribution fit are given in the first and the second row, respectively. See the legend to Fig. 2 C for experimental details and Materials and Methods for the technique.

* With the exception of lysozyme and barstar, the rest of the proteins possess only one trp residue.

$\ddagger$ Mean lifetime $= \sum_{i=1}^{N} \alpha_i \tau_i / \sum_{i=1}^{N} \alpha_i$, where N is 2 or 3 for discrete exponential fit and $N = 150$ for distribution fit.

the lifetimes are close to each other. A priori, this method will not be suitable for samples where the fluorophore distribution may be extensively heterogeneous. The use of MEM gives a continuous distribution of lifetimes as the required solution without assuming any model or mathematical function to describe the distribution of lifetimes. The distribution obtained by MEM is a general one that includes also the solution obtained in a discrete multiexponential analysis. If the decay is truly a sum of N exponentials (representing N species), then the MEM analysis generates a distribution of lifetimes with N peaks (approximately gaussian shaped (Swaminathan and Periasamy, unpublished)), provided the signal-to-noise ratio is adequate in the data to resolve the peaks. Thus, the distribution solution by MEM ought to be consistent with the results obtained in a multiexponential fit if both the solutions are acceptable for the fluorescence decay data. A good fit of the fluorescence decay data by both the methods implies a good agreement in the value of the mean lifetime. This was found to be true, within 10% deviation, for .the fluorescence decay data of all the samples for which the results obtained by both the methods are given in Tables 1–3. Our experimental results indicate that the distribution of lifetimes is not unimodal for any protein, native or denatured. The distribution is either bimodal or trimodal.

There are other methods of fitting the fluorescence data to a distribution of lifetimes. The exponential series method has been tested to produce distributions that are similar to those obtained by MEM (Siemiarczuk et al., 1990). Another popular method is based on prior knowledge about the distribution

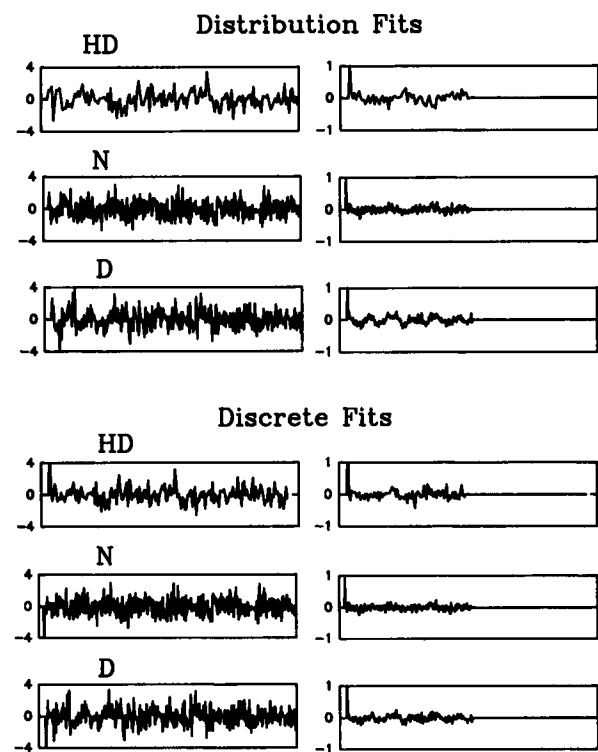**Distribution Fits**

Discrete Fits

FIGURE 3   Residual (left) and autocorrelation (right) distributions obtained after fitting the fluorescence intensity decays of melittin (shown in Fig. 1 A) to a discrete sum of exponentials and a distribution of lifetimes given by the maximum entropy method. The decay parameters are given in Tables 1, 2, and 3, respectively. The symbols N, D, and HD stand for the same conditions as described in Fig. 1 A.

of lifetimes. This method assumes the number of peaks in the distribution (unimodal, bimodal, etc.) and the shape of the distribution function (Lorentzian, Gaussian, etc.; Alcala et al., 1987a,b). The method has been widely used for the analysis of fluorescence data of proteins in the native and denatured states (Rosato et al., 1990; Mei et al., 1992; Bismuto et al., 1988, 1991; Fernando and Royer, 1992; Gryczynski et al., 1988). The use of a Lorentzian function for the distribution was sought to be justified based on a model of distribution of fluorophore in a continuously varying microenvironment (Alcala et al., 1987a). However, the validity of this model for proteins has not been tested adequately.

MEM makes no assumptions about the distribution shape or the number of modes, and hence, there is no bias to any particular physical model or mathematical equation for the distribution. If the distribution of lifetimes is truly unimodal, MEM ought to have returned that distribution as final. This was not the case in any of the proteins in the native or in the random coil state. The distributions were either bimodal or trimodal in all. We examined the time-resolved fluorescence decay of melittin in the denatured state (6 M GdnHCl at 25°C) for various data acquisition conditions to see if we could ever recover a unimodal distribution as the MEM solution. Indeed, we were able to get such a unimodal distribution when the time-resolved fluorescence decay was poor in signal-to-noise ratio. The fluorescence decays of melittin in the presence of GdnHCl (6 M) were collected at a time resolution of 37.8 ps/channel for different peak counts, 1000, 5000, 10,000, and 20,000. The total counts in each of these decay profiles were 8.2×10^4, 4.2×10^5, 8.5×10^5, 1.7×10^6 counts, respectively. Since the statistics of noise distribution in fluorescence counting are well known (the standard deviation being $\sqrt{N}$ where N is the photons counted) the signal-to-noise ratios at the peak of their emission are ~31, ~71, ~100, and ~141, respectively. Analysis of the decays by MEM gave distributions of lifetimes as shown in Fig. 4. As seen in Fig. 4, a unimodal distribution could be obtained only if the peak count is 1000 or less. Resolution of an additional peak begins to show up at improved, higher signal-to-noise ratio.

We examined also the feasibility of fitting the time-resolved fluorescence decay data directly to a unimodal Lorentzian distribution function. The fit was found to be adequate for the data set with 1000 counts at the peak, but the fits were increasingly poor for the data sets with higher peak counts. The results are summarized in Table 4. It was noted that the mean lifetime and full width at half maximum were nearly the same for all data sets. However, the high χ^2 value and the nonrandom distribution of weighted residuals (not shown) are sufficiently strong evidence that the unimodal Lorentzian function is not supported by the data. Thus, we conclude that a good fit of the unimodal Lorentzian distribution lifetimes is an artifact of insufficient information in the fluorescence data.

The most significant feature of the lifetime distribution patterns presented in Fig. 2, A–C is the similarity of the patterns for most of the proteins in their denatured state at 25°C
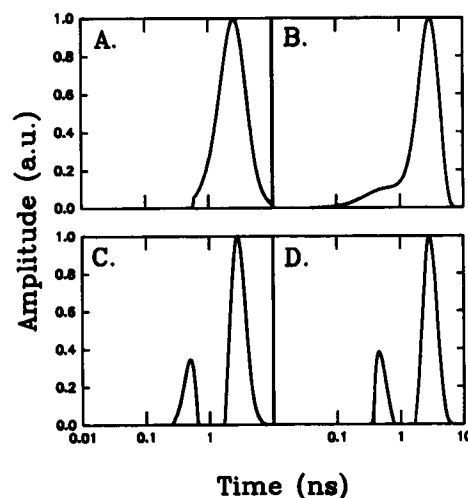

FIGURE 4 Fluorescence lifetime distributions for denatured melittin (at 25°C and pH 7.0 in the presence of 6 M GdnHCl, 10 mM NaH$_2$PO$_4$, and 1 mM EDTA) obtained in MEM analysis of the decays (37.8 ps/channel) for the following peak counts: (A) 1000; (B) 5000; (C) 10,000; (D) 20,000. The χ^2 values for the distribution fits are (A) 1.04; (B) 1.01; (C) 1.16; (D) 1.13.

TABLE 4 Parameters obtained by fitting the fluorescence intensity decays of melittin to a unimodal Lorentzian distribution

Peak counts	Γ^* (ns)	τ_m (ns)	χ^2
1000	1.09	2.46	1.08
5000	0.93	2.60	1.37
10,000	0.98	2.60	2.13
20,000	0.99	2.57	2.84

See the legend to Fig. 4 for experimental details.
* Full width at half maximum.

(Fig. 2 B) and 85°C (Fig. 2 C), when compared with the dissimilar patterns obtained for the native state (Fig. 2 A). The common features for most of the denatured proteins is the bimodal (at 25°C) or trimodal (at 85°C) distribution of qualitatively similar shapes and relative amplitudes. These common features in the distribution of lifetimes suggest common structure, which is the random coil state of the protein. There are, however, exceptions to the generality. For example, in the presence of the denaturant, the distribution for monellin at 25°C is trimodal with an extra peak at 6.4 ns and the distribution for superoxide dismutase at 85°C is bimodal. In addition, there are substantial quantitative deviations among the similar distribution patterns. For the distributions at 25°C these deviations are 1) resolution of the peaks (the peaks in subtilisin Carlsberg were not resolved), 2) position of the peaks, 3) average lifetimes and amplitudes (see Table 2), and 4) the global average lifetime τ_m (which varies from 1.57 to 2.66 ns). Similar quantitative deviations are also observable in the distribution patterns at 85°C. These deviations are attributable to the sequence specificity of the protein in the random coil state.

Interestingly, the quantitative and qualitative results of the distribution of lifetimes for the multi-trp proteins lysozyme and barstar in their denatured state (6 M GdnHCl) are

also similar (distributions not shown) to those of the single-trp proteins. This indicates that the multi-trp proteins are also in their random coil state and the different trps in the same polypeptide chain have similar fluorescence decay characteristics.

Indeed, one would expect that the fluorescence decay of the trp residue in any polypeptide to be identical if the polypeptide is in the truly random coil state. However, marginal differences in the fluorescence decay could arise depending upon the location of the trp residue (Chen et al., 1987) in the chain and the neighboring residues. For example, quencher groups (e.g., sulfhydryl or carboxyl) in the adjacent residue may reduce the lifetime of indole (Demchenko, 1992). A trp at the end of the chain may be more dynamic than one in the middle of the chain. Certain protein-specific features may also be responsible for some deviations. For example, in lysozyme containing six trps the energy transfer quenching is possible even in the random coil state. In superoxide dismutase the tight binding of the metal ion (Zn^{2+} or Cu^{2+}) in the random coil state could quench the fluorescence. These factors can explain the quantitative variations in the decay parameters for the single- and multi-trp proteins in the random coil state.

There has been extensive work on the assignment of the multiple lifetimes of trp in proteins and polypeptides (Beechem and Brand, 1985; Tanaka and Mataga, 1992; Swaminathan et al., 1994). The two fluorescence lifetimes for the free trp in water has been assigned to the rotamer structures about the C_α—C_β bond, which makes the indole group proximal to the carboxyl group in two of the three structures (Szabo and Rayner, 1980). The rotamer structures themselves are estimated to be long-lived (upper limit of time constant $\sim10^3$ s^{-1}) in nuclear magnetic resonance (NMR) experiments (Ross et al., 1992), and hence the rotamer structures would show up as distinctly different species in the nanosecond time scale fluorescence experiments. The fluorescence decay of a trp analog that has restricted rotation about the C_α—C_β bond is biexponential, which correlated with the two conformational population derived from NMR (Colucci et al., 1990; McMahon et al., 1992). The combined study of fluorescence decay and NMR of trp containing polypeptide has shown that the population of the three rotamers derived from NMR experiments were in excellent correlation with the amplitudes of the three fluorescence decay components (Ross et al., 1992). In view of all these previous studies one can reasonably conclude that the bimodal distributions of lifetimes of trp observed for the proteins in their random coil state at 25°C (Fig. 2 *B* and Table 2) are to be assigned to three populations of the rotamer structures, of which two rotamer configurations have similar fluorescence decay characteristics. However, the validity of the alternate model of excited state relaxation, which would associate the bimodal distribution with unrelaxed and relaxed excited states of indole, is not ruled out by the results at 25°C.

The distribution of lifetimes changes from bimodal to trimodal at 85°C in the presence of the denaturant. This is an interesting feature of the random coil state. In these cases the results obtained by the discrete three-exponential analysis were in excellent agreement with the average lifetimes and amplitudes obtained for the trimodal distributions. These observations go well with the rotamer model, where one can argue that the averaging effect of the two rotamers at 25°C is removed at 85°C. On the other hand, the model of excited state relaxation will have to invoke an additional relaxation intermediate. We believe that the trimodal distribution at 85°C is yet another strong argument in favor of the rotamer model.

An interesting feature of the results obtained for the denatured proteins at 85°C is the higher lifetime value for one of the three components than that of indole or NATA at the same temperature (Table 3). This feature is noticed in the results at 25°C only for monellin (Table 2). The three lifetimes at 85°C are ~0.2, ~0.7 and ~1.3 ns and their amplitudes are ~0.3, ~0.65, and ~0.05, respectively. The lifetimes of NATA and indole in the presence of 6 M GdnHCl are as follows: NATA, 2.85 ns at 25°C and 0.75 ns at 85°C; and indole, 3.50 ns at 25°C and 0.73 ns at 85°C. It is difficult to account for the higher lifetime of 1.3 ns for the indole in the random coil state of the polypeptide. However, the amplitude for this component is small. Interestingly, a higher value (1.06 ns) was also observed in the case of trp under similar conditions (85°C, 6 M GdnHCl), the fluorescence decay of which was biexponential (0.53 ns and 1.06 ns with amplitudes of 0.77 and 0.23, respectively).

A question that needs to be addressed is the physical significance of the shape and width of the peaks in the bimodal and trimodal distributions of lifetimes obtained in MEM analysis. Does the shape and width of the individual components of the distribution indicate a continuous variation of the microenvironment of the fluorophore? Such an association of shape and width is physically meaningful, important information and hence, care should be taken to eliminate other possible explanations for the shape and width of the distribution. It is known that MEM analysis of synthetic fluorescence data and that of standard samples (indole, NATA, trp, rhodamines), which are known to be cases of one or two exponential decay functions, give unimodal and bimodal distributions (Livesey and Brochon, 1987; Swaminathan and Periasamy, unpublished). The resolvability of the bimodal distribution depends upon the signal-to-noise ratio. When resolved, the distribution is approximately gaussian in the log τ space. More importantly, the width of the distribution is dependent on the information content (the signal-to-noise ratio or the peak count) in the fluorescence decay. Thus, the distribution width is either a genuine indication of the heterogeneity of microenvironment and lifetimes or an indication of insufficient information in the fluorescence data for a fluorophore in homogeneous environment having a single lifetime. The distribution of lifetimes obtained for the denatured proteins in the random coil state at 25 and 85°C are examined in light of the above general observations. In all trimodal distributions at 85°C the peaks are well resolved and

the distribution is resolvable as a superposition of three gaussians (in the log τ space), with the exception of superoxide dismutase (the third peak at $\sim$1 ns is not resolved well). The width of the individual components (Fig. 2 C), especially the middle one, which is also the most dominant one, is relatively constant in all except myelin. It is less likely that the distributions of lifetimes indicate a continuous distribution of microenvironment. It is more plausible that the widths of the component peaks in the trimodal distribution at 85°C are indications of limitation of information in the data. The fluorescence decay is essentially a three-exponential function corresponding to the three rotamer structures.

The distribution of lifetimes at 25°C in the presence of denaturant is bimodal for all the proteins except monellin (Fig. 2 B). This similarity of distributions is strong evidence that the protein is unfolded to a random coil state. However, the bimodal distributions were not identical in all. Unlike the results of proteins in the native form or those of denatured ones at 85°C, there is an important difference in the results of discrete exponential analysis and those of distribution analysis. The distributions are bimodal for all except monellin, whereas a two-exponential fit was not adequate for any of the single-trp proteins. However, the average lifetime, which is a measure of the quantum yield calculated from both the fits, is nearly the same. The average lifetimes are not the same for all. This could indicate the importance of local structural properties near the trp region. It is now believed that unfolding of the proteins by denaturants need not lead to a completely random coil state of the polypeptide. Residual structures, especially those that pertain to very early folding intermediates, may persist in an otherwise random coil state. These residual structures may not be large enough to be detected in circular dichroism but detectable in NMR experiments (Neri et al., 1992). It has been found that a small segment of polypeptide (5–6 residues, including a trp) can form a hydrophobic cluster in urea denaturation of 434-repressor protein (Neri et al., 1992). Trp, being an aromatic amino acid, could also be a nucleation center for hydrophobic structure formation. The fluorescence property of trp is therefore highly susceptible to the identity of the neighboring residues. There is very little information at present on the effect of neighboring residues on the fluorescence of trp. The quantitative differences in the decay parameters observed for

the denatured proteins, which are apparently in their random coil state, may be attributed to differences in the local structure. In contrast to the results at 25°C, the average lifetimes (and other decay parameters) for denatured proteins at 85°C are relatively closer to each other. It appears that the local structures at 25°C are destroyed at high temperature, and the polypeptide is truly in the random coil state at 85°C.

The results for cyclic hexapeptide are worth discussing as a special case because this does not have secondary or tertiary structures in the "native" form, and this molecule cannot form a random coil under any condition. The residues adjacent to trp (see Table 5 for the sequence) do not have long side chains (like leucine) for structure-forming hydrophobic interaction with indole. The distribution of lifetimes is trimodal, and the discrete exponential fit indicated a three-exponential function. Three lifetimes are also found in other trp-containing small polypeptides (Ito et al., 1993; Chen et al., 1991). These three lifetimes are attributable to the rotamer states. In the presence of 6 M GdnHCl the distribution becomes bimodal and the average lifetime decreases from 1.78 to 1.58 ns, indicating quenching interaction of indole with GdnHCl. However, 6 M GdnHCl does not quench the fluorescence of NATA or that of trp (the lifetime(s) are about the same as in the absence of GdnHCl), but the fluorescence of indole is quenched (the lifetime decreases from 4.38 to 3.50 ns). The quenching mechanism is not clear at present. To understand this quenching mechanism it is necessary to have quenching data for several trp-containing dipeptides and tripeptides.

We now come to the interesting question of the physical significance of the multimodal distributions of lifetimes in proteins in their native state. Multimodal distribution is an indication of one of the following situations: 1) rotamer states for trp residue, 2) long-lived microstates or conformations of the protein in which the local environments near the trp residue are different, and 3) in the case of multi-trp proteins, differences in the local environment of trp residues. A combination of these three factors could also be envisaged in some cases. In situations where only case (1) is operative, the distribution may have a maximum of three peaks (trimodal) corresponding to the three rotamer populations. Multimodal (above three) distribution of lifetimes is an unambiguous

TABLE 5 Details regarding the amino acid sequences flanking the tryptophan residue and the position of trp in the polypeptide chain in the nine single-trp proteins studied

Protein	Local sequence*	$\lambda_{max}^{emission}$	Chain length
Glucagon	—Val-Gln-Trp$_{14}$-Leu-Met—	354	29
Cyclic hexapeptide	—Gly-Gly-Trp-Arg-Phe-His—	350	6
Human albumin	—Lys-Ala-Trp$_{213}$-Ala-Val—	344	585
Melittin	—Ile-Ser-Trp$_{19}$-Ile-Lys—	352	26
Monellin	Gly-Glu-Trp$_3$-Glu-Ile— (Chain B)	344	45(A) + 50(B)
Basic myelin	—Phe-Ser-Trp$_{115}$-Gly-Ala—	351	169
Subtilisin Carlsberg	—Ile-Glu-Trp$_{112}$-Ala-Thr—	354	274
Ribonuclease T$_1$	—Tyr-Glu-Trp$_{59}$-Pro-Ile—	328	104
Superoxide dismutase	—Lys-Val-Trp$_{32}$-Gly-Ser—	346	153

The fluorescence emission maximum on excitation at 295 nm is also listed for the native condition (pH 7.0, 25°C).

* Protein sequences were obtained from the SWISS-PROT protein sequence databank (Bairoch and Boeckmann, 1992).

indication for the presence of more than one microstate or conformation of the protein, as observed in apocytochrome c (Vincent et al., 1988). None of the single-trp proteins studied by us has given distributions beyond trimodal.

The distribution of lifetimes for the single-trp proteins in the native state (Fig. 2 A) shows considerable variation in the profiles. Among these, the profiles for glucagon, melittin, and RNase T1 appear similar but the structural or spectroscopic details differ substantially for these three. Table 5 gives the sequence details in the neighborhood of trp residue, the fluorescence emission maxima, and the chain length as the number of amino acid residues. The emission maximum at 328 nm in RNase T1 suggests that the trp residue is buried inside, which is confirmed in the x-ray structure (Heinemann and Saenger, 1982), but the red-shifted emission in glucagon and melittin suggests that the tryptophan is solvent exposed. There is no obvious correlation between the macroscopic structural and spectroscopic details of the proteins and the observed lifetime distributions that are determined by the microscopic structure and dynamics in the trp region. The bimodal and trimodal distributions for the native proteins can be resolved into two or three gaussian profiles, each of which may be thought to represent a lifetime component. Unlike the distributions for denatured proteins, the width of the gaussian profiles varies substantially among the proteins in the native state. The width indicates either a genuinely heterogeneous microenvironment near the trp residue or the limitation of information in the fluorescence data. Resolution of this dilemma requires a systematic study of fluorescence decays of selected proteins, like human albumin, at various peak counts and time resolutions. This work is in progress.

REFERENCES

Alcala, J. R., E. Gratton, and F. G. Prendergast. 1987a. Fluorescence lifetime distributions in proteins. Biophys. J. 51:597–604.

Alcala, J. R., E. Gratton, and F. G. Prendergast. 1987b. Interpretation of fluorescence decays in proteins using continuous lifetime distributions. Biophys. J. 51:925–936.

Bairoch, A., and B. Boeckmann. 1992. The SWISS-PROT protein sequence databank. Nucleic Acids Res. 20:2019–2022.

Banker, K. V., V. R. Bhagat, R. Das, S. Doraiswamy, A. S. Ghangrekar, D. S. Kamat, N. Periasamy, V. J. P. Srivatsavoy, and B. Venkataraman. 1989. Techniques for the study of fast chemical processes with half-times of the order of microseconds or less. Indian J. Pure Appl. Phys. 27: 416–428.

Beechem, J. M., and L. Brand. 1985. Time-resolved fluorescence in proteins. Annu. Rev. Biochem. 54:43–71.

Bevington, P. R. 1969. Data Reduction and Error Analysis for the Physical Sciences. McGraw-Hill Inc., New York.

Bismuto, E., E. Gratton, and G. Irace. 1988. Effect of unfolding on the tryptophanyl fluorescence lifetime distribution in apomyoglobin. Biochemistry. 27:2132–2136.

Bismuto, E., I. Sirangelo, and G. Irace. 1991. Conformational dynamics of unfolded peptides as a function of chain length: a frequency domain fluorescence approach. Arch. Biochem. Biophys. 291:38–42.

Chang, M. C., J. W. Petrich, D. B. McDonald, and G. R. Fleming. 1983. Nonexponential fluorescence decay of tryptophan, tryptophylglycine and glycyltryptophan. J. Am. Chem. Soc. 105:3819–3824.

Chen, L. X.-Q., J. W. Petrich, G. R. Fleming, and A. Perico. 1987. Picosecond fluorescence studies of polypeptide dynamics: fluorescence anisotropies and lifetimes. Chem. Phys. Lett. 139:55–61.

Chen, R. F., J. R. Knutson, H. Ziffer, and D. Porter. 1991. Fluorescence of tryptophan dipeptides: correlations with rotamer model. Biochemistry. 30:5184–5195.

Colucci, W. J., L. Tilstra, M. C. Sattler, F. R. Fronczek, and M. D. Barkley. 1990. Conformational studies of a constrained tryptophan derivative: implications for the fluorescence quenching mechanism. J. Am. Chem. Soc. 112:9182–9190.

Creed, D. 1984. The photophysics and photochemistry of the near-uv absorbing amino acids-I. Tryptophan and its simple derivatives. Photochem. Photobiol. 39:537–562.

Demchenko, A. P. 1992. Fluorescence and dynamics in proteins. In Topics in Fluorescence Spectroscopy, Vol. 3, Biochemical Applications. J. R. Lakowicz, editor. Plenum Press, New York. 65–111.

Eftink, M. R. 1991. Fluorescence techniques for studying protein structure. In Methods of Biochemical Analysis, Vol. 35. C. H. Suelter, editor. Wiley, New York. 127–205.

Fernando, T., and C. A. Royer. 1992. Unfolding of trp repressor studied using fluorescence spectroscopic techniques. Biochemistry. 31:6683–6691.

Grinvald, A., and I. Z. Steinberg. 1974. On the analysis of fluorescence decay kinetics by the method of least-squares. Anal. Biochem. 59: 583–598.

Grinvald, A., and I. Z. Steinberg. 1976. The fluorescence decay of tryptophan residues in native and denatured proteins. Biochim. Biophys. Acta. 427:663–678.

Gryczynski, I., M. Eftink, and J. R. Lakowicz. 1988. Conformation heterogeneity in proteins as an origin of heterogeneous fluorescence decays, illustrated by native and denatured ribonuclease T_1. Biochim. Biophys. Acta. 954:244–252.

Heinemann, U., and W. Saenger. 1982. Specific protein-nucleic acid recognition in ribonuclease T1–2′-guanylic acid complex: an x-ray study. Nature. 299:27–31.

Ito, A. S., A. M. L. Castrucci, V. J. Hruby, M. E. Hadley, D. T. Krajcarski, and A. G. Szabo. 1993. Structure-activity correlations of melanotropin peptides in model lipids by tryptophan fluorescence studies. Biochemistry. 32:12264–12272.

Lakowicz, J. R. 1983. Principles of Fluorescence Spectroscopy. Plenum Press, New York.

Livesey, A. K., and J. C. Brochon. 1987. Analyzing the distribution of decay constants in pulse-fluorimetry using maximum entropy method. Biophys. J. 52:693–706.

Lumry, R., and M. Hershberger. 1978. Status of indole photochemistry with special reference to biological application. Photochem. Photobiol. 27: 819–840.

McMahon, L. P., W. J. Colucci, M. L. McLaughlin, and M. D. Barkley. 1992. Deuterium isotope effects in constrained tryptophan derivatives: implications for tryptophan photophysics. J. Am. Chem. Soc. 114: 8442–8448.

Mei, G., N. Rosato, N. Silva, R. Rusch, E. Gratton, I. Savini, and A. Finazzi-Agro. 1992. Denaturation of human Cu/Zn superoxide dismutase by guanidine hydrochloride: a dynamic fluorescence study. Biochemistry. 31:7224–7230.

Neri, D., M. Billeter, G. Wider, and K. Wuthrich. 1992. NMR determination of residual structure in a urea-denatured protein, the 434-repressor. Science. 257:1559–1563.

Periasamy, N., S. Doraiswamy, G. B. Maiya, and B. Venkataraman. 1988. Diffusion controlled reactions: fluorescence quenching of cationic dyes by charged quenchers. J. Chem. Phys. 88:1638–1651.

Petrich, J. W., M. C. Chang, D. B. McDonald, and G. R. Fleming. 1983. On the origin of nonexponential fluorescence decay in tryptophan and its derivatives. J. Am. Chem. Soc. 105:3824–3832.

Rosato, N., E. Gratton, G. Mei, and A. Finazzi-Agro. 1990. Fluorescence lifetime distributions in human superoxide dismutase. Biophys. J. 58: 817–822.

Ross, J. B. A., H. R. Wyssbrod, R. A. Porter, G. P. Schwartz, C. A. Michaels, and W. R. Laws. 1992. Correlation of tryptophan fluorescence intensity decay parameters with ^{1}H NMR-determined rotamer conformations: [tryptophan][2]oxytocin. Biochemistry. 31:1585–1594.

Siemiarczuk, A., B. D. Wagner, and W. R. Ware. 1990. Comparison of the maximum entropy and exponential series methods for the recovery of distributions of lifetimes from fluorescence lifetime data. J. Phys. Chem. 94:1661–1666.

Skilling, J., and R. K. Bryan. 1984. Maximum entropy image reconstruction: general algorithm. *Mon. Not. R. Astr. Soc.* 211:111–124.

Swaminathan, R., N. Periasamy, J. B. Udgaonkar, and G. Krishnamoorthy. 1994. Molten globule-like conformation of barstar: a study by fluorescence dynamics. *J. Phys. Chem.* 98:9270–9278.

Szabo, A. G., and D. M. Rayner. 1980. Fluorescence decay of tryptophan conformers in aqueous solution. *J. Am. Chem. Soc.* 102:554–563.

Tanaka, F., and N. Mataga. 1992. Non-exponential decay of fluorescence of tryptophan and its motions in proteins. *In* Dynamics and Mechanisms of Photoinduced Transfer and Related Phenomena. N. Mataga, T. Okada, and H. Masuhara, editors. Elsevier Science Publishers, New York. 501–512.

Vekshin, N., M. Vincent, and J. Gallay. 1992. Excited-state lifetime distributions of tryptophan fluorescence in polar solutions. Evidence for solvent exciplex formation. *Chem. Phys. Lett.* 199: 459–464.

Vincent, M., J. C. Brochon, F. Merola, W. Jordi, and J. Gallay. 1988. Nanosecond dynamics of horse heart apocytochrome c in aqueous solution as studied by time-resolved fluorescence of the single tryptophan residue (trp-59). *Biochemistry.* 27:8752–8761.

Weber, G. 1953. Rotational brownian motion and polarization of the fluorescence solutions. *In* Advances in Protein Chemistry, Vol. 8. M. L. Anson, K. Bailey, and J. T. Edsall, editors. Academic Press, New York. 415–459.